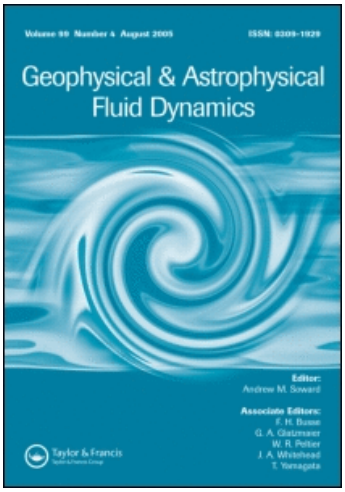


**Geophysical & Astrophysical Fluid Dynamics**
Publication details, including instructions for authors and subscription information:
http://www.informaworld.com/smpp/title~content=t713642804

# Parity coupling in $\alpha^2$-dynamos

Rainer Hollerbach[ab]
[a] Institute of Geophysics and Planetary Physics, Scripps Institution of Oceanography, La Jolla, CA, USA [b] Department of Mathematics and Statistics, University of Newcastle upon Tyne, UK

**To cite this Article** Hollerbach, Rainer(1991) 'Parity coupling in $\alpha^2$-dynamos', Geophysical & Astrophysical Fluid Dynamics, 60: 1, 245 — 260
**To link to this Article: DOI:** 10.1080/03091929108220005
**URL:** http://dx.doi.org/10.1080/03091929108220005

*Geophys. Astrophys. Fluid Dynamics*, Vol. 60, pp. 245–260
Reprints available directly from the publisher
Photocopying permitted by license only



# PARITY COUPLING IN $\alpha^2$-DYNAMOS

RAINER HOLLERBACH*

*Institute of Geophysics and Planetary Physics, Scripps Institution of Oceanography, La Jolla, CA 92093 USA*

(*Received 12 December 1990*)

The modal $\alpha^2$-dynamo of Hollerbach and Ierley (1991) is extended to include both parities, dipolar and quadrupolar. Two choices of $\alpha$ are considered. As before, the solutions approach the Taylor state, and the subsequent equilibration is independent of the viscosity in the asymptotic limit. The first choice of $\alpha$ yields stable steady-state pure-parity solutions of either type, and may yield some insight into the question of parity selection. The second choice of $\alpha$ yields rather complex time-dependent mixed-parity solutions, and demonstrates the extent to which parity coupling can affect the evolution of time-dependent solutions.

KEY WORDS: Parity coupling, $\alpha^2$-dynamos, Taylor's constraint.



## 1. INTRODUCTION

In an earlier paper, Hollerbach and Ierley (1991), hereafter referred to as HI, considered dipole solutions to a modal $\alpha^2$-dynamo in the limit of asymptotically small viscosity. The reason for focusing on dipole solutions was that all known planetary dynamos are predominantly dipolar. This fact is somewhat puzzling in view of the observation of Roberts (1972), that for typical choices of $\alpha$ the linear critical eigenvalues for the onset of dynamo action are only slightly greater for quadrupole symmetry than for dipole symmetry. Indeed, by considering a slightly modified "comparison problem" with exactly degenerate eigenvalues, Proctor (1977) showed that this is to be expected as a general result. He therefore conjectured that the observed preference for dipole parity might be caused by the presence of some (unspecified) large-scale mean flow, which would break the degeneracy.

The aim of this paper is to investigate that conjecture by considering the effect that the large-scale flow set up by one parity type has on the other. The two parity types separate in the sense that a solution of pure parity of either type will remain so even in the nonlinear regime. They do not separate in the sense that there is no interaction between them; a flow set up by either will react back on both. Thus, instead of merely comparing uncoupled linear eigenvalues, we consider the nonlinearly coupled evolution of both parities simultaneously. The form of the modal amplitude equations derived in HI is however unchanged, one merely allows for quadrupole as well as dipole modes.

*Present address: Department of Mathematics and Statistics, University of Newcastle upon Tyne, Newcastle upon Tyne, NE1 7RU UK.

Because of the complexity introduced by having more modes, only two choices of $\alpha$ are investigated here:

$$\alpha=\alpha_0\frac{729}{16}r^8(1-r^2)^2\cos\theta, \tag{1.1}$$

as in Section 5 of HI, and

$$\alpha=\alpha_0\cos\theta, \tag{1.2}$$

as the limiting case $q_1\to\infty$ in Sections 6 and 7 of HI. As before, the first yields steady-state solutions, while the second yields time-dependent solutions.

The remainder of this paper is organized as follows: Section 2 reviews the basic equations and extends the derivation of the modal amplitude equations given in HI. Section 3 discusses the basic nature of the parity coupling. Section 4 implements (1.1) and investigates in some detail the approach to the Taylor state, and the subsequent inviscid equilibration, of the two pure-parity solutions. Section 5 implements (1.2) and investigates the quite complex mixed-parity time-dependent solutions which result. Finally, Section 6 summarizes the main results.



## 2. MODAL AMPLITUDE EQUATIONS

The scaled mean-field equations of HI are

$$\frac{\partial\mathbf{B}}{\partial t}=\nabla\times(\mathbf{U}\times\mathbf{B})+\nabla\times(\alpha\mathbf{B})+\nabla^2\mathbf{B}, \tag{2.1}$$

$$2\hat{\mathbf{k}}\times\mathbf{U}=-\nabla p+(\nabla\times\mathbf{B})\times\mathbf{B}-E\mathbf{U}, \tag{2.2}$$

$$\nabla\cdot\mathbf{B}=\nabla\cdot\mathbf{U}=0, \tag{2.3}$$

where $\mathbf{B}$ is the large-scale magnetic field forced by the $\alpha$-effect, $\mathbf{U}$ is the large-scale velocity induced by the Lorentz force, and $p$ is the pressure.

Note that for the asymptotically small frictional term I am once again using linear friction, see Salmon (1986). Since the introduction of this term has generated a certain amount of controversy, a few comments are in order: Taylor's constraint depends only on the particular property of the Coriolis force that its contribution enters (2.6a) as $2\psi_z$, which vanishes when integrated in $z$ and evaluated using the no-normal-flow boundary condition. A common misconception among advocates of the traditional friction $+E\nabla^2\mathbf{U}$ seems to be that the Taylor constraint depends somehow on the Ekman boundary layer. That is simply false. It is true that for that particular friction the precise details of how the geostrophic flow is determined are intimately coupled with the details of the boundary layer, but the existence of the Taylor constraint does not depend on the existence of the

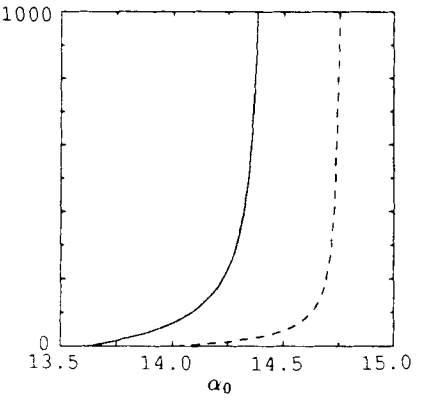


**Figure 1** The equilibrium energy, as a function of $\alpha_0$, incorporating only the geostrophic flow. The stable dipole is solid, the unstable quadrupole is dashed.

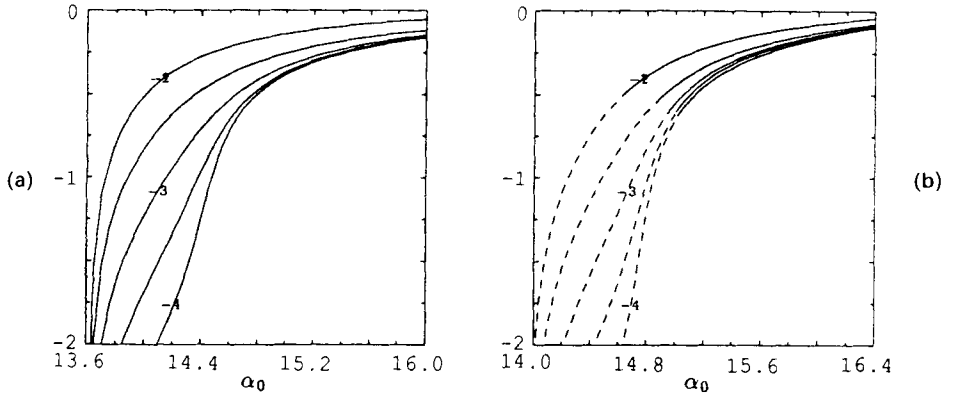


**Figure 2** The logarithm of the equilibrium energy, as a function of $\alpha_0$, incorporating the geostrophic and next-order ageostrophic flow, for viscosities $E$ from $10^{-2}$ to $10^{-4}$. (a) Dipole. (b) Quadrupole.

boundary layer. The boundary layer exists because for that particular friction the order of the equation is reduced in the limit of vanishing viscosity. It is precisely to avoid this extraneous complication that the simpler linear friction is introduced.

Returning to (2.1) and (2.2), and decomposing as

$$\mathbf{B} = B(r,\theta)\hat{\mathbf{e}}_\phi + \nabla \times [A(r,\theta)\hat{\mathbf{e}}_\phi], \tag{2.4a}$$

$$\mathbf{U} = v(r,\theta)\hat{\mathbf{e}}_\phi + \nabla \times [\psi(r,\theta)\hat{\mathbf{e}}_\phi], \tag{2.4b}$$

the induction equation (2.1) becomes

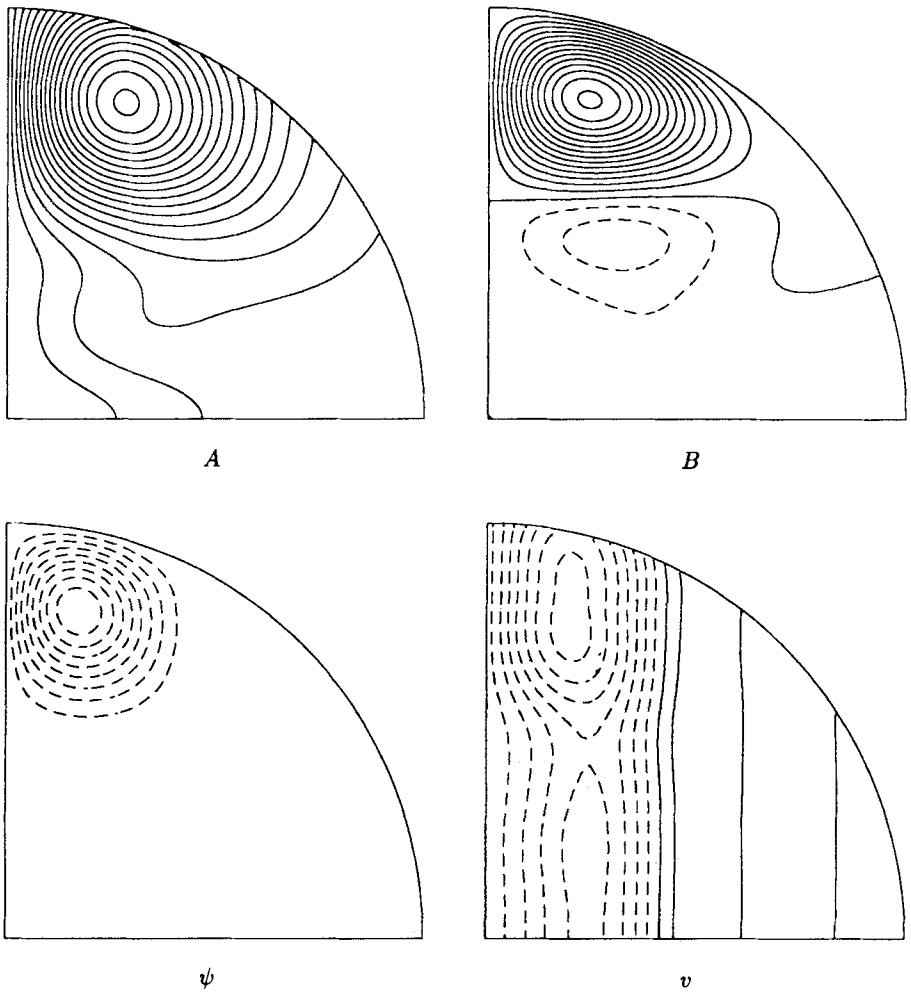


**Figure 3** The spatial structure of the inviscidly equilibrated dipole and the associated flow at $\alpha_0 = 16.0$. The contour intervals of $\psi$ are 0.05, and of $v$ are 1, so the flow is still somewhat less than $\alpha$.

$$\frac{\partial A}{\partial t} = N(\psi, A) + \alpha B + D^2 A, \tag{2.5a}$$

$$\frac{\partial B}{\partial t} = M(v, A) - M(B, \psi) + \nabla \times [\alpha \nabla \times (A\hat{\mathbf{e}}_\phi)] \cdot \hat{\mathbf{e}}_\phi + D^2 B, \tag{2.5b}$$

and the momentum equation (2.2) becomes

$$2\psi_z - Ev = -N(B, A), \tag{2.6a}$$

$$2v_z + ED^2\psi = M(B, B) + M(D^2 A, A), \tag{2.6b}$$

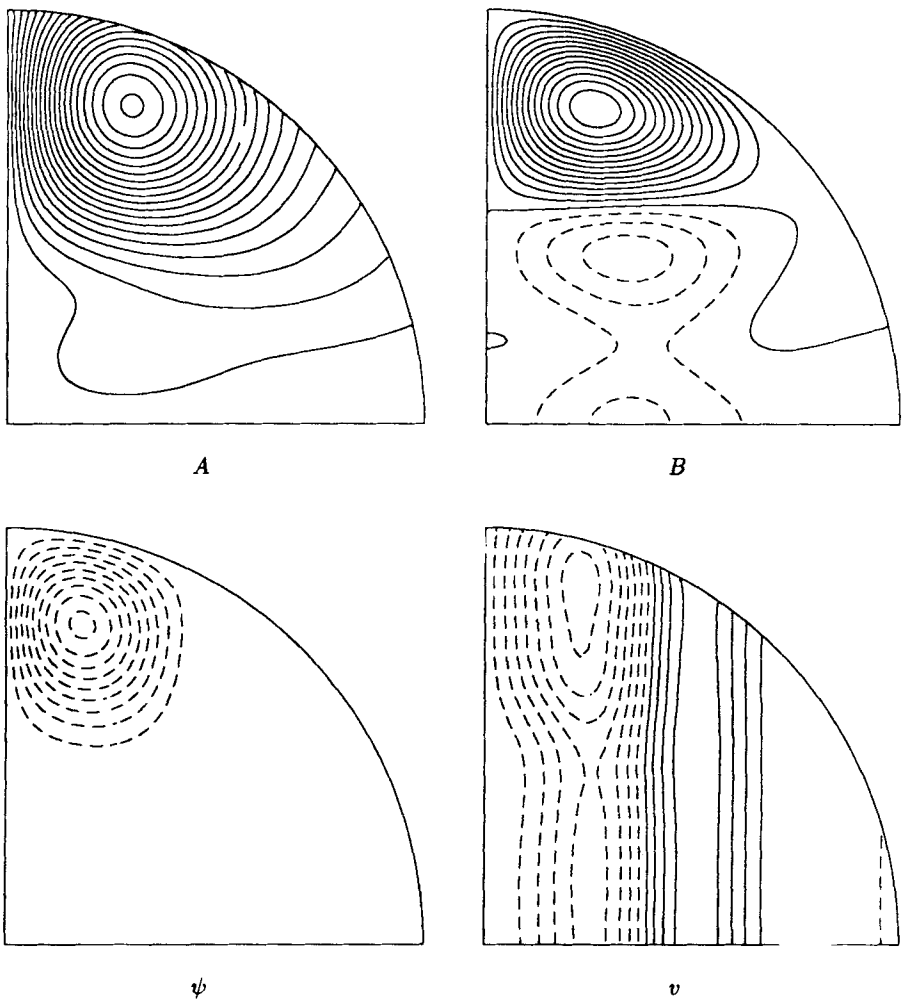


**Figure 4** The spatial structure of the inviscidly equilibrated quadrupole and the associated flow at $\alpha_0 = 16.4$. The contour intervals of $\psi$ are 0.05, and of $v$ are 1, so the flow is still somewhat less than $\alpha$.

where

$$D^2 = \nabla^2 - (r \sin\theta)^{-2}, \tag{2.7}$$

$$N(x, y) = \hat{\mathbf{e}}_\phi \cdot [\nabla \times (x\hat{\mathbf{e}}_\phi) \times \nabla \times (y\hat{\mathbf{e}}_\phi)], \tag{2.8}$$

$$M(x, y) = \hat{\mathbf{e}}_\phi \cdot \nabla \times [(x\hat{\mathbf{e}}_\phi) \times \nabla \times (y\hat{\mathbf{e}}_\phi)]. \tag{2.9}$$

As in HI, (2.6) can be solved as an asymptotic expansion in powers of $E$,

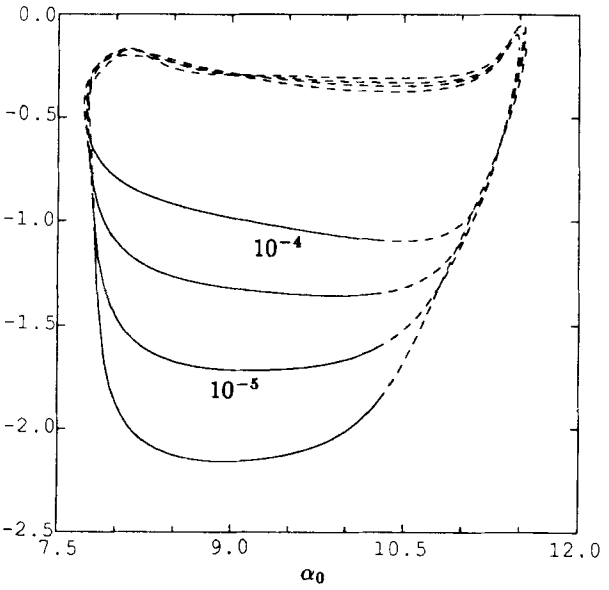


**Figure 5** The logarithm of the equilibrium energy, as a function of $\alpha_0$, incorporating the geostrophic and next-order ageostrophic velocity, for viscosities $E$ from $10^{-4}$ to $10^{-5.5}$. Note the absence of any stable inviscid equilibration.

$$v=\frac{1}{E}v_g(\rho)+[v_0(\rho,z)+v_0'(\rho)]+E[v_1(\rho,z)+v_1'(\rho)]+\cdots, \tag{2.10a}$$

$$\psi=\psi_0(\rho,z)+E\psi_1(\rho,z)+\cdots, \tag{2.10b}$$

where the geostrophic flow turns out to be

$$v_g=\frac{1}{2z_T}\int_{-z_T}^{+z_T}N(B,A)\,dz=-\frac{1}{2\rho^2(1-\rho^2)^{1/2}}\frac{d}{d\rho}\left[\rho^2\int_{-z_T}^{+z_T}BA_z\,dz\right]. \tag{2.11}$$

For the next-order ageostrophic corrections one gets

$$\psi_0=\tfrac{1}{2}\int_{-z_T}^{z}[v_g-N(B,A)]\,dz, \tag{2.12a}$$

$$v_0=\tfrac{1}{2}\int_{0}^{z}[M(B,B)+M(D^2A,A)]\,dz, \tag{2.12b}$$

$$v_0'=-\frac{1}{2z_T}\int_{-z_T}^{+z_T}v_0\,dz, \tag{2.12c}$$

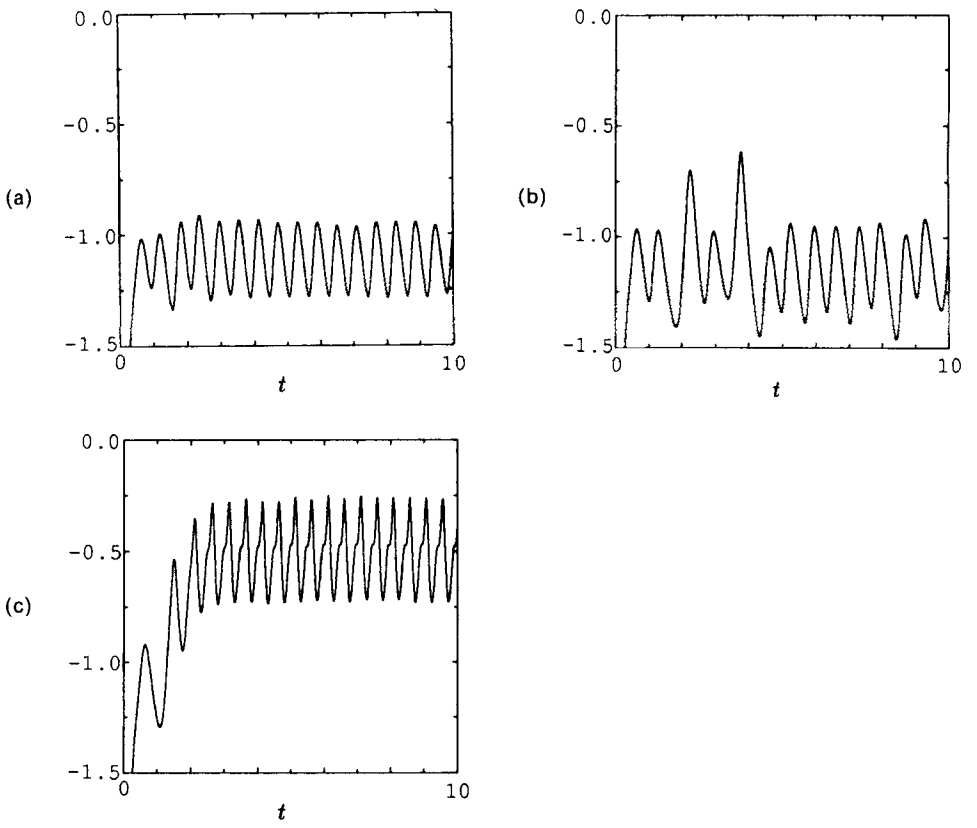


**Figure 6** The logarithm of the energy as a function of time. (a) $\alpha_0 = 10.60$. (b) $\alpha_0 = 10.65$. (c) $\alpha_0 = 10.70$. All at $E = 10^{-5}$.

where $\pm z_T = \pm(1-\rho^2)^{1/2}$ are the top and bottom boundaries of the spherical dynamo. Note that the lower limits of integration in (2.11), (2.12a), and (2.12c) are no longer 0, as in HI, since we are no longer assuming any particular symmetry about the equator.

Next, the free decay eigenmodes of (2.5) are

$$A = \exp(-\lambda^2 t) P_l^{(1)}(\cos\theta)\, j_l(\lambda r), \qquad j_{l-1}(\lambda) = 0, \tag{2.13a}$$

$$B = \exp(-\lambda^2 t) P_l^{(1)}(\cos\theta)\, j_l(\lambda r), \qquad j_l(\lambda) = 0, \tag{2.13b}$$

where the eigenvalues $\lambda$ are determined by the boundary conditions that $A$ match to a potential field and $B$ match to zero. For dipole modes, $l$ is odd for $A$ and even for $B$, and the opposite for quadrupole modes. Arranging the modes in order of increasing $\lambda$, that is, in order of increasing free decay rate, it turns out that the dipole modes naturally come in sets of $n^2$, $\frac{1}{2}n(n+1)$ for $A$ and $\frac{1}{2}n(n-1)$ for $B$, and the quadrupole modes naturally come in sets of $n(n-1)$, $\frac{1}{2}n(n-1)$ for both $A$ and $B$. In this work I have used 25 dipole and 20 quadrupole modes. Various

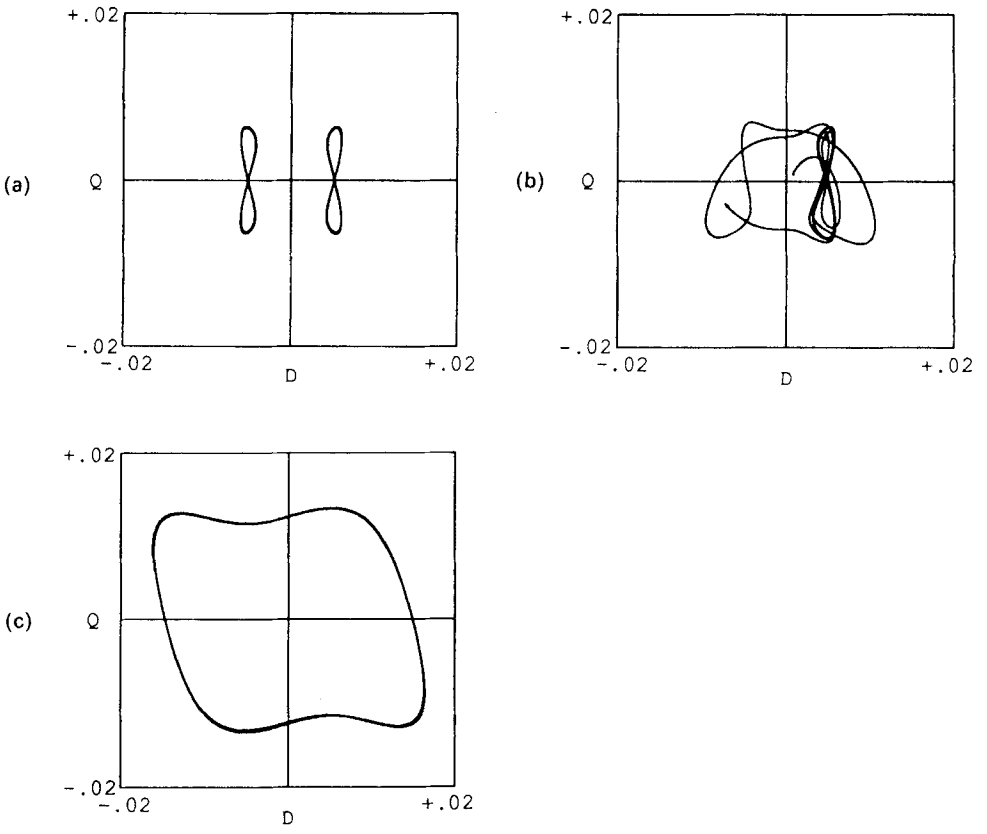


**Figure 7** The trajectory of the evolution in the phase space of $a_{1_Q}$ versus $a_{1_D}$. (a) $\alpha_0 = 10.60$. (b) $\alpha_0 = 10.65$. (c) $\alpha_0 = 10.70$. All at $E = 10^{-5}$.

experiments were also done varying the level of truncation, to verify that the results are representative of the full dynamics, but will not be reported here. See Section 5 of HI for a discussion of the level of truncation.

So, expanding the fields as

$$A = \sum a_i(t) A_i(r, \theta), \qquad B = \sum b_i(t) B_i(r, \theta), \tag{2.14}$$

in (2.5), with the flow given by (2.11) and (2.12), one gets a set of amplitude equations of the form

$$\frac{da_i}{dt} = -\lambda_{a_i}^2 a_i + \alpha_0 C_{ij}^{(1)} b_j + C_{ijkl}^{(4)} a_j a_k b_l, \tag{2.15a}$$

$$\frac{db_i}{dt} = -\lambda_{b_i}^2 b_i + \alpha_0 C_{ij}^{(2)} a_j + E^{-1} C_{ijkl}^{(3)} a_j b_k a_l + C_{ijkl}^{(5)} b_j a_k b_l + C_{ijkl}^{(6)} a_j a_k a_l. \tag{2.15b}$$

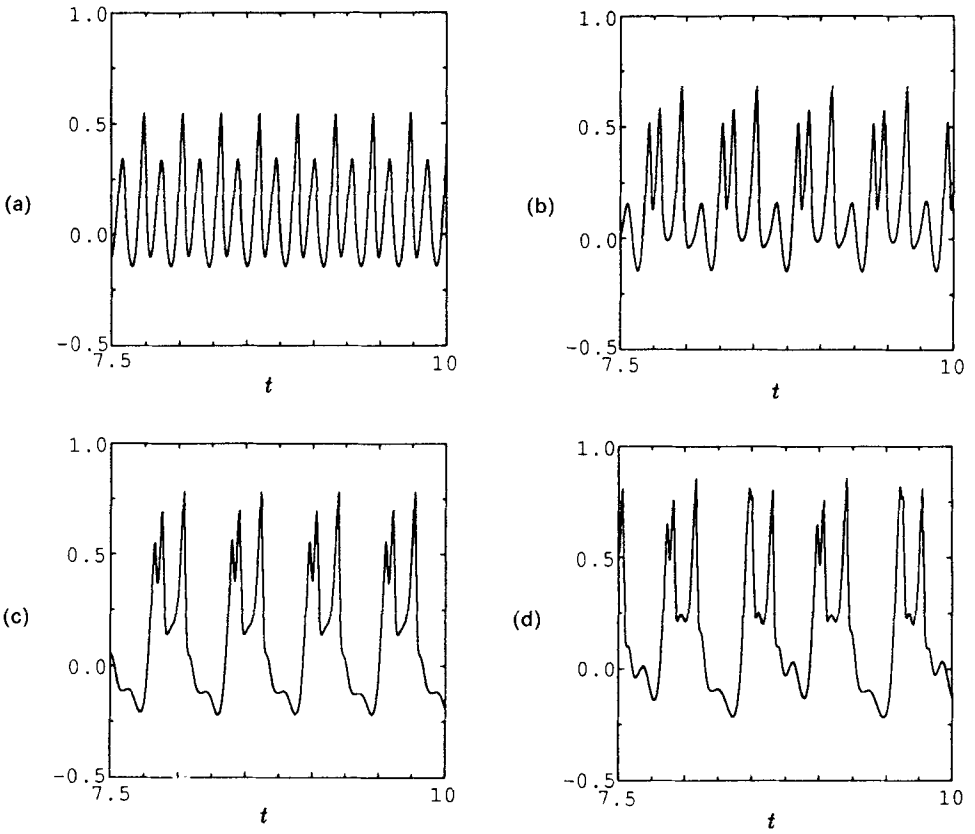


**Figure 8** The logarithm of the energy as a function of time. (a) $\alpha_0 = 11.60$. (b) $\alpha_0 = 11.75$. (c) $\alpha_0 = 11.90$. (d) $\alpha_0 = 11.963$. All at $E = 10^{-5}$.

The coefficient arrays $C^{(1)}$ through $C^{(6)}$ are simply the projections of the various terms onto this modal set. And unlike in HI, the modal set now includes all the modes, not just the dipole modes. The basic form of the modal equations (2.15) is however unchanged.

## 3. DISCUSSION

With no loss in generality, one can separate an arbitrary magnetic field into so-called dipole fields, having $A$ symmetric and $B$ antisymmetric about the equator, and quadrupole fields, having $A$ antisymmetric and $B$ symmetric. For the geophysically relevant case of $\alpha$ antisymmetric about the equator, the $\alpha$-effect forcing in (2.5) will indeed couple only the two dipole components and the two quadrupole components separately, with no cross-coupling between the two parity types.

In the nonlinear regime, we need to include the large-scale flow induced by the

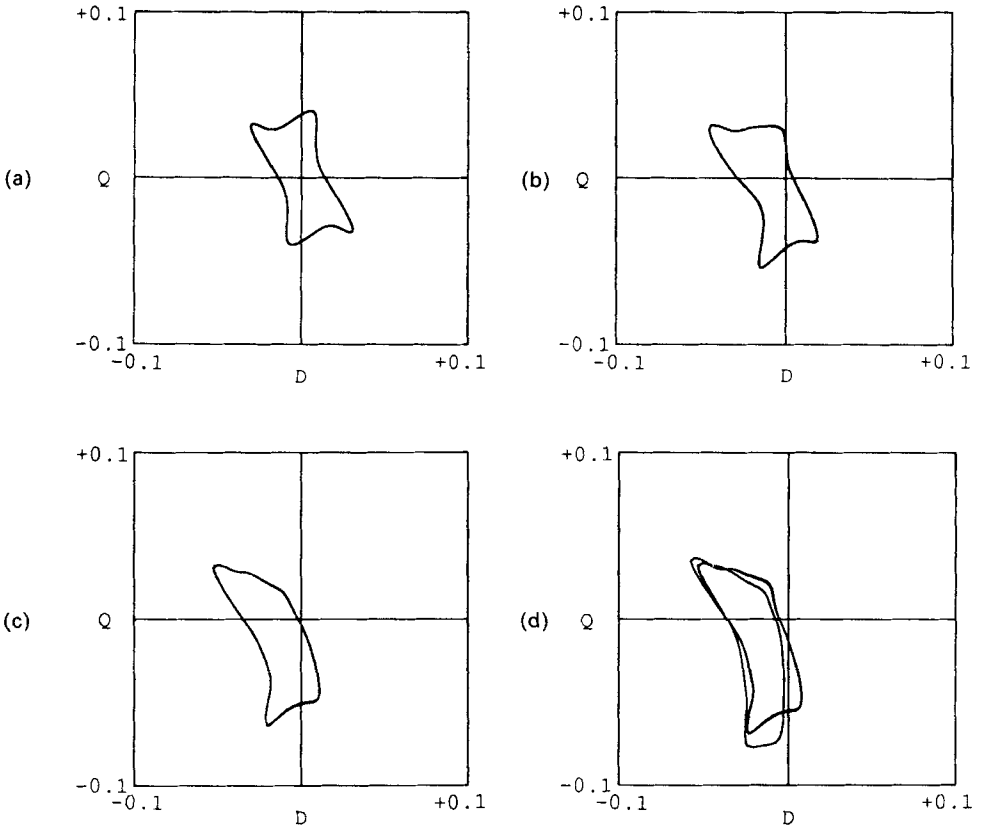


**Figure 9** The trajectory of the evolution in the phase space of $a_{1_Q}$ versus $a_{1_D}$. (a) $\alpha_0 = 11.60$. (b) $\alpha_0 = 11.75$. (c) $\alpha_0 = 11.90$. (d) $\alpha_0 = 11.963$. All at $E = 10^{-5}$.

Lorentz force. Since this force is quadratic in **B**, both pure-parity fields will set up the same parity in the flow, namely one with $v$ symmetric and $\psi$ antisymmetric. Such a flow, once set up by either parity field, will clearly react back on both. However, it will not change the parity of the field, in the sense that it will react on a dipole to yield a dipole, and on a quadrupole to yield a quadrupole.

In addition to this coupling, there is also the coupling of the two parity types to set up a flow having the opposite parity from that set up by either type alone. (Note, however, that by its symmetry this flow is limited to the ageostrophic terms since the geostrophic component $v_g$ is necessarily symmetric about the equator.) This flow will then react back to couple the two types, reacting on a dipole to yield a quadrupole and vice versa.

Letting $D$ denote dipole modes (both $a_i$ and $b_i$), and $Q$ denote quadrupole modes, the schematic structure of the modal amplitude equations (2.15) is

$$\frac{dD}{dt} = L(D) + C(D^3) + C(DQ^2), \tag{3.1a}$$

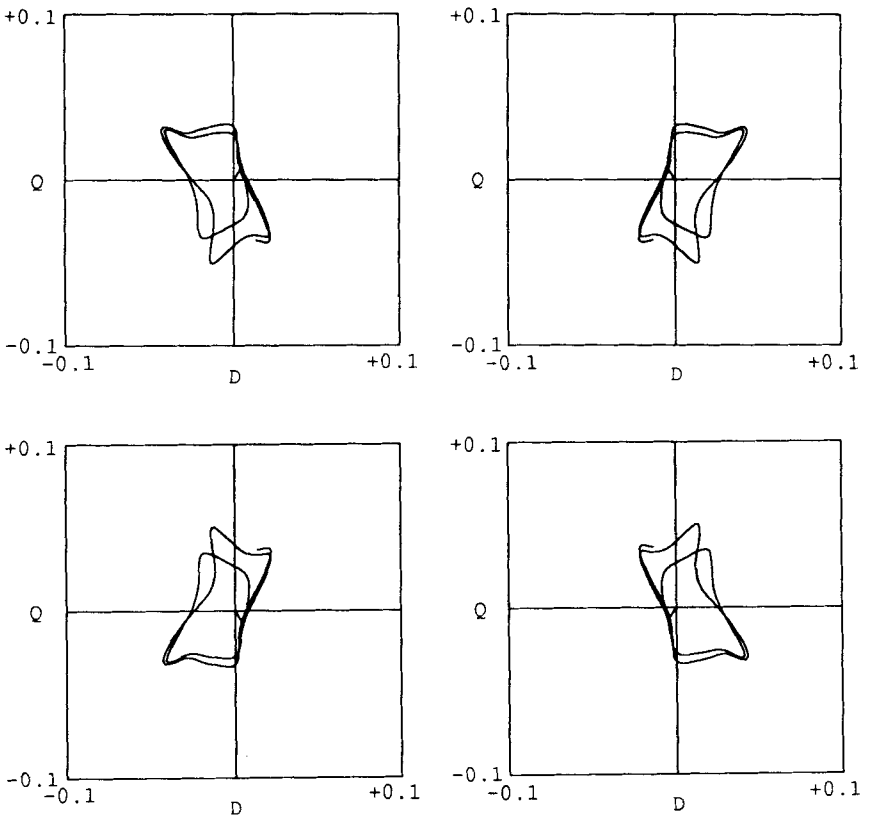


**Figure 10** The four possible states available at $\alpha_0 = 11.75$.

$$\frac{dQ}{dt} = L(Q) + C(Q^3) + C(QD^2), \tag{3.1b}$$

where the $L$ are the linear terms and the $C$ are the cubically nonlinear terms. The "missing" terms [$L(Q)$, $C(D^2Q)$, $C(Q^3)$ in (3.1a), $L(D)$, $C(Q^2D)$, $C(D^3)$ in (3.1b)] are absent precisely because the two parities interact only as described above. The corresponding entries in the coefficient arrays $C^{(1)}$ through $C^{(6)}$ in (2.15) are identically zero.

Note that the dipole modes $D$ and the quadrupole modes $Q$ in (3.1) are coupled only through the nonlinear terms. Thus, the linear eigenvalues given by Roberts are indeed completely uncoupled, and correspond to pure-parity eigensolutions. Furthermore, these pure-parity solutions will remain so, even in the nonlinear regime, since one can consistently set either $D$ or $Q$ identically equal to zero in (3.1) and consider only the evolution of the other parity type by itself, as was done in HI with pure dipole solutions. All of these solutions will continue to exist in the full system (3.1), but they may now interact with the opposite parity as well. (They may, for example, be unstable with respect to a perturbation of the opposite

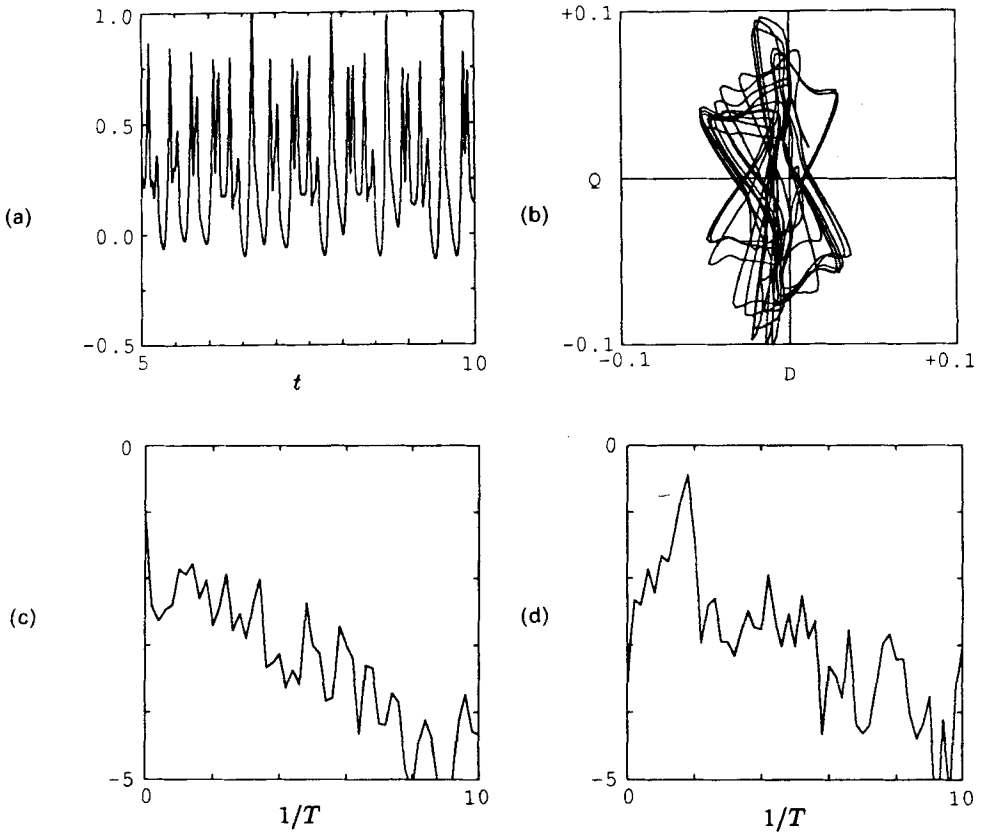


**Figure 11** The chaotic solution at $\alpha_0 = 12$, $E = 10^{-5}$. (a) The logarithm of the energy as a function of time. (b) The trajectory of the evolution in the phase space of $a_{1_Q}$ versus $a_{1_D}$. (c) and (d) The logarithm of the power spectra, as a function of inverse-period, of $a_{1_D}$ and $a_{1_Q}$, respectively.

parity, and some complicated mixed-parity evolution may result.) It is this coupling between the two parity types which is the subject of this paper.

Finally, an important property of (3.1) is that for a given solution, one can change the sign of either $D$ or $Q$ *independently* and still have a solution. That is, for a given field and associated flow satisfying the dynamo equations, one can reverse the dipole and quadrupole components of the field *separately* and still have a solution. (Of course, the component of the flow due to the direct coupling of the two parities will also reverse accordingly.) This symmetry property will be of interest in Section 5.

## 4. STEADY-STATE SOLUTIONS: $\alpha = \alpha_0(729/16)\, r^8(1-r^2)^2 \cos\theta$

As in HI, for 25 dipole modes the linear eigenvalue is 13.6. In addition, for 20 quadrupole modes the linear eigenvalue is 14.0. Thus, both parities are excited

with almost equal ease, in agreement with Roberts' results. When $\alpha_0$ is increased beyond the critical eigenvalue, the solutions again evolve from the infinitesimal linear solutions until the increased dissipation associated with the geostrophic flow balances the increased forcing and equilibrates the field. But, as mentioned earlier, each solution preserves its parity even in the nonlinear regime; in this case the coupling between the modes affects only their stability with respect to one another. Figure 1 shows the equilibrium energies incorporating only the gestrophic flow, with the dipole solid and the quadrupole dashed. It is evident that both solutions approach the Taylor state, the dipole at 14.4 and the quadrupole at 14.8. Thus, not only are the linear eigenvalues $\alpha_c$ very close, but more importantly so are the nonlinear eigenvalues $\alpha_T$. ($\alpha_T$ is more important than $\alpha_c$ because the Taylor regime is of greater geophysical interest than the viscously controlled regime.) The observed preference for dipole symmetry is thus all the more puzzling.

The answer ought to be to look at the linear stability of these solutions: I stated above that solid indicates the dipole, and dashed indicates the quadrupole. I could equally well have stated that solid indicates stability, and dashed indicates instability. Both solutions are stable with respect to themselves, that is, the dipole with respect to a dipole-type perturbation, and the quadrupole with respect to a quadrupole-type perturbation. However, whereas the dipole is also stable with respect to a quadrupole perturbation, the quadrupole is unstable with respect to a dipole perturbation. Thus, although the eigenvalues are indeed quite close together, the dipole completely suppresses the quadrupole, and the final equilibration will inevitably be a pure dipole solution.

Alas, this happy state of affairs does not persist into the Taylor regime. As Figure 2 shows, beyond $\alpha_T$ the inclusion of the ageostrophic terms once again leads to an inviscid equilibration. However, the stability characteristics are now such that both solutions are stable: the quadrupole gains stability via a pitchfork bifurcation to an unstable mixed mode. Thus, while the system certainly has a strong preference for a pure parity state, it will not necessarily choose the "right" one; depending upon which (mixed) initial conditions one chooses, one can end up with either a pure dipole or a pure quadrupole. Either of these states will then persist, totally suppressing the other. Figures 3 and 4 show the corresponding fields and the flows associated with them. Note how remarkably similar the fields are; except for slight adjustments at the equator required by their differing symmetries they are almost identical. Evidently the dynamo processes in the two hemispheres are only very weakly coupled, so that reversing the field in only one hemisphere (and thereby changing the parity) has little effect on its structure and on the magnitudes of the eigenvalues. Note also that the magnitude of the flow is still less than $\alpha$, so the small-scale flow (of which $\alpha$ is a parameterization) still dominates the total flow.

## 5. TIME-DEPENDENT SOLUTIONS: $\alpha = \alpha_0 \cos\theta$

Attention will focus in this section on the time-dependent behavior observed in the strongly nonlinear regime. Of course, the weakly nonlinear solutions in Figure 7a

of HI continue to exist, as do corresponding quadrupole solutions. Also, the linear eigenvalues are once again quite close: the 25-mode dipole has $\alpha_{c_1}=7.66$, $\alpha_{c_2}=11.17$; the 20-mode quadrupole has $\alpha_{c_1}=7.84$, $\alpha_{c_2}=11.34$. However, the solutions arising out of all of these are of limited interest.

The first interesting result comes from re-examining the stability of the loops in Figure 8 of HI, this time allowing not only dipole- but also quadrupole-type perturbations. One notices in Figure 5 that the inviscid solution arising out of the second vertical asymptote of the Taylor-type solution is now also unstable. There is thus no stable inviscid equilibration. Therefore, since neither parity is stable with respect to the presence of the other, one would expect some time-dependent mixed-parity behavior to result.

This is precisely what occurs. After the viscously controlled lower portion of the loop loses stability via a Hopf bifurcation to a quadrupole perturbation, one gets a series of limit cycles of gradually increasing amplitude as one proceeds beyond the bifurcation point. Figures 6 and 7 show, respectively, the energy as a function of time (starting from infinitesimal initial conditions), and the evolution in the phase space of the first quadrupole mode $a_{1_Q}$ versus the first dipole mode $a_{1_D}$. For $\alpha_0=10.60$ one gets relatively small fluctuations about either of the possible polarities $\pm D$. By the time $\alpha_0=10.70$ the fluctuations are large enough for the field to reverse polarity. Also, these results are almost inviscid, that is, they are only very weakly dependent on $E$ in the asymptotic limit, roughly to the same extent as the pure dipole loops of Figure 5 are at these $\alpha_0$'s. One might expect that for even smaller $E$ these results would be completely independent of viscosity, but one cannot quite reach that regime numerically.

The onset of oscillatory solutions is thus quite different from what it was for the pure dipole solutions of HI. The precise nature of the transition, such as whether it is supercritical or subcritical, is not however investigated here, for want of sufficient computer time. Also, the possibility that other initial conditions might yield other limit cycles was not exhaustively investigated, since these time-dependent runs are extremely lengthy. The intermediate run at $\alpha_0=10.65$ indicates that the transition may be rather complicated, or at least may take a long time to settle into one or the other of the simpler states.

Turning now to the symmetry property discussed earlier, namely that for a given solution both the dipole and the quadrupole components can reverse their respective polarities independently, one notices that depending on initial conditions, the $\alpha_0=10.60$ solution will end up in either of the distinct states $+D\pm Q$ or $-D\pm Q$, but within each state, reversing $Q$ yields the same state. In contrast, the $\alpha_0=10.70$ solution will end up in either of the distinct states $\pm(D+Q)$ or $\pm(D-Q)$, but within each state reversing both $D$ and $Q$ together yields the same state. This behavior will become even more interesting as we increase $\alpha_0$ further.

Figures 8 and 9 show the behavior for larger $\alpha_0$. It is evident that nothing fundamental has changed in going from 10.70 to 11.60, except that the amplitudes have increased, and the solutions are now completely independent of viscosity. By 11.75, however, another symmetry-breaking bifurcation has occurred, and the state $+(D+Q)$ is no longer equivalent to $-(D+Q)$. There are thus four distinct states available, and Figure 10 shows how appropriate choice of initial conditions will

yield all four. (It is obviously not very difficult; one merely reverses the signs of the infinitesimal initial components. It does, however, serve to demonstrate the truth of the assertion that $\pm D \pm Q$ is a solution, and furthermore that this symmetry is properly implemented in the modal amplitude equations by noting that certain of the coupling coefficients are identically zero by precisely this symmetry.)

Returning to Figures 8 and 9, associated with the symmetry-breaking bifurcation, one notices an apparent doubling of the period in the energy. The actual period of the evolution has not changed, however. Before the bifurcation, each half of the evolution looks the same in the energy figure, and so the energy has half the true periodicity, but after the bifurcation each half looks distinct, and so the energy has the true periodicity. However, if one increases $\alpha_0$ even further, by 11.963 a true period-doubling bifurcation has occurred.

By $\alpha_0 = 12$ one has chaos, although it still appears to be asymmetric, that is, not all four possible polarity configurations are present equally frequently. There would appear to be (at least) two distinct chaotic regions in phase space, symmetric regarding $\pm Q$ but asymmetric regarding $\pm D$. Of course, these remarks concerning the (a)symmetry in the chaotic regime are really only speculative, since one cannot run the system long enough to make statistically reliable statements about the relative frequencies of the four polarities. Nevertheless, since there are the four distinct period-doublings, one might expect that immediately after the onset of chaos one will still have four distinct regions, which presumably coalesce first to two and then to one.



## 6. CONCLUSIONS

The results of Section 4 would seem to support Proctor's conjecture that the presence of a large-scale flow can very effectively suppress a particular solution, although it is rather disappointing that the flows we have considered, namely those set up by the solutions themselves, can suppress either parity. To explain the preference for dipole over quadrupole parity may thus require the presence of some other flow, driven by some other (unspecified) effect.

The results of Section 5 turn out not to address the question of parity selection at all, since both parities are present in essentially equal amplitudes. Instead, the most important conclusion probably lies simply in noting the contrast between the rich variety of time-dependent solutions in this case, compared with the relative sparsity (no symmetry breaking, no period doubling, no chaos) in the pure dipole case of HI (although one cannot rule out such behaviour if the system were forced harder). Evidently parity coupling can have a significant impact on the time-dependent evolution, and any dynamo theorists wishing to understand features of that evolution, like the chaotic reversals of the geodynamo, would probably be wise not to restrict their models to dipole symmetry *a priori*, even though the geodynamo is predominantly dipolar.

*Acknowledgements*

As a graduate student I was partially funded by grants OCE86-01399 and OCE89-01720 from the

National Science Foundation. I thank my adviser Glenn Ierley for his continual support and advice. I also thank Bill Young for providing the computing facilities.

## *References*

Hollerbach, R. and Ierley, G. R., "A modal $\alpha^2$-dynamo in the limit of asymptotically small viscosity," *Geophys. Astrophys. Fluid Dynam.* **56,** 133–158 (1991).

Proctor, M. R. E., "The role of mean circulation in parity selection by planetary magnetic fields," *Geophys. Astrophys. Fluid Dynam.* **8,** 311–324 (1977).

Roberts, P. H., "Kinematic dynamo models," *Phil. Trans. R. Soc. Lond.* A **272,** 663–698 (1972).

Salmon, R., A simplified linear ocean circulation theory," *J. Mar. Res.* **44,** 695–711 (1986).